

**Ancillary files for “Observation of Beam Spin Asymmetries in the
Process $ep \rightarrow e'\pi^+\pi^-X$ with CLAS12”**

CLAS Collaboration

I. BEAM SPIN ASYMMETRIES

The extracted asymmetry values for all seven azimuthal modulations in each bin are given in Tables I-VI. The listed asymmetry amplitudes have been corrected for the beam polarization and, if desired, can be further corrected for the relevant twist-2 or twist-3 kinematic depolarization factors defined in Refs [1–3],

$$K_2 \equiv \frac{C(\epsilon, y)}{A(\epsilon, y)}, \quad (1)$$

$$K_3 \equiv \frac{W(\epsilon, y)}{A(\epsilon, y)}, \quad (2)$$

with

$$A(\epsilon, y) \equiv \frac{y^2}{2(1-\epsilon)} = \frac{1}{1+\gamma^2} \left(1 - y + \frac{1}{2}y^2 + \frac{1}{4}\gamma^2y^2 \right), \quad (3)$$

$$C(\epsilon, y) \equiv \frac{y^2}{2(1-\epsilon)} \sqrt{1-\epsilon^2} = \frac{y}{\sqrt{1+\gamma^2}} \left(1 - \frac{1}{2}y \right), \quad (4)$$

$$W(\epsilon, y) \equiv \frac{y^2}{2(1-\epsilon)} \sqrt{2\epsilon(1-\epsilon)} = \frac{y}{\sqrt{1+\gamma^2}} \sqrt{1 - y - \frac{1}{4}\gamma^2y^2}. \quad (5)$$

Values are reported as percentages (the asymmetry multiplied by 100) with the statistical uncertainty as a superscript and the systematic uncertainty as a subscript: $A_{\text{LU}}^{\text{stat}}_{\text{sys}}$.

Bin	$\langle x \rangle$	$A_{LU}^{\sin(\phi_h)}$	$A_{LU}^{\sin(\phi_h - \phi_{R\perp})}$	$A_{LU}^{\sin(\phi_{R\perp})}$	$A_{LU}^{\sin(2\phi_h - \phi_{R\perp})}$	$A_{LU}^{\sin(2\phi_h - 2\phi_{R\perp})}$	$A_{LU}^{\sin(-\phi_h + 2\phi_{R\perp})}$	$A_{LU}^{\sin(3\phi_h - 2\phi_{R\perp})}$
1	0.105	1.03 ± 0.54	-2.42 ± 0.45	1.30 ± 0.51	-0.80 ± 0.48	1.84 ± 0.47	-2.39 ± 0.43	0.69 ± 0.42
2	0.127	2.28 ± 0.54	-2.23 ± 0.47	2.03 ± 0.51	-0.61 ± 0.48	1.65 ± 0.48	-1.26 ± 0.44	1.25 ± 0.42
3	0.143	1.84 ± 0.54	-1.58 ± 0.49	2.50 ± 0.51	-1.00 ± 0.48	1.12 ± 0.49	-1.36 ± 0.45	0.62 ± 0.43
4	0.157	2.63 ± 0.52	-1.70 ± 0.49	2.58 ± 0.50	-0.21 ± 0.47	0.76 ± 0.49	-1.05 ± 0.45	0.83 ± 0.42
5	0.174	2.22 ± 0.48	-2.03 ± 0.46	2.72 ± 0.46	-1.15 ± 0.43	1.83 ± 0.46	-2.60 ± 0.41	0.88 ± 0.39
6	0.191	1.74 ± 0.51	-1.85 ± 0.50	2.37 ± 0.49	-1.72 ± 0.46	1.61 ± 0.49	-1.78 ± 0.44	-0.15 ± 0.41
7	0.211	2.58 ± 0.45	-1.23 ± 0.46	2.00 ± 0.44	-1.26 ± 0.41	1.71 ± 0.45	-1.68 ± 0.40	0.53 ± 0.38
8	0.235	1.51 ± 0.47	-1.09 ± 0.48	2.46 ± 0.45	-1.01 ± 0.43	1.24 ± 0.47	-1.53 ± 0.42	0.45 ± 0.39
9	0.261	2.09 ± 0.49	-0.56 ± 0.52	1.76 ± 0.47	-0.62 ± 0.45	1.62 ± 0.50	-1.24 ± 0.45	1.06 ± 0.41
10	0.294	1.52 ± 0.45	-0.77 ± 0.50	2.22 ± 0.44	-1.20 ± 0.43	0.82 ± 0.47	-1.56 ± 0.42	0.02 ± 0.39
11	0.342	3.61 ± 0.46	-2.05 ± 0.52	3.26 ± 0.45	-1.21 ± 0.44	1.07 ± 0.49	-1.62 ± 0.43	-0.08 ± 0.40
12	0.441	2.49 ± 0.46	0.10 ± 0.54	2.03 ± 0.45	-0.77 ± 0.45	0.40 ± 0.50	-0.68 ± 0.45	0.70 ± 0.41

TABLE I: The mean value of x and the final beam spin asymmetries as a function of x in each bin for each of the seven azimuthal modulations. Asymmetries are given as $100A_{LU}^{\text{stat}}$.

Bin	$\langle M_h \rangle$	$A_{LU}^{\sin(\phi_h)}$	$A_{LU}^{\sin(\phi_h - \phi_{R\perp})}$	$A_{LU}^{\sin(\phi_{R\perp})}$	$A_{LU}^{\sin(2\phi_h - \phi_{R\perp})}$	$A_{LU}^{\sin(2\phi_h - 2\phi_{R\perp})}$	$A_{LU}^{\sin(-\phi_h + 2\phi_{R\perp})}$	$A_{LU}^{\sin(3\phi_h - 2\phi_{R\perp})}$
1	0.338	3.46 ± 0.45	0.21 ± 0.84	1.32 ± 0.65	0.20 ± 0.61	-2.07 ± 0.83	0.67 ± 0.61	-1.32 ± 0.61
2	0.422	2.64 ± 0.52	2.18 ± 0.78	-0.70 ± 0.65	0.03 ± 0.57	-1.59 ± 0.75	0.83 ± 0.56	0.14 ± 0.54
3	0.496	2.07 ± 0.61	2.65 ± 0.81	-0.08 ± 0.72	0.33 ± 0.59	-1.39 ± 0.78	0.27 ± 0.60	-0.39 ± 0.55
4	0.568	2.36 ± 0.62	0.69 ± 0.73	0.94 ± 0.70	-1.19 ± 0.55	-1.96 ± 0.71	-0.14 ± 0.57	-0.22 ± 0.50
5	0.641	1.48 ± 0.63	2.08 ± 0.67	0.64 ± 0.66	-0.64 ± 0.52	1.22 ± 0.64	-1.74 ± 0.53	1.16 ± 0.47
6	0.708	2.07 ± 0.57	-1.20 ± 0.56	1.79 ± 0.56	-1.52 ± 0.47	2.25 ± 0.54	-1.89 ± 0.46	0.15 ± 0.41
7	0.759	2.25 ± 0.59	-2.62 ± 0.57	2.57 ± 0.56	-0.85 ± 0.49	4.36 ± 0.55	-3.26 ± 0.48	0.82 ± 0.42
8	0.805	2.07 ± 0.56	-2.98 ± 0.52	2.58 ± 0.52	-0.93 ± 0.47	4.21 ± 0.51	-2.24 ± 0.45	0.26 ± 0.41
9	0.864	2.36 ± 0.50	-3.51 ± 0.46	2.45 ± 0.45	-0.22 ± 0.42	2.00 ± 0.45	-1.91 ± 0.41	0.32 ± 0.38
10	0.939	0.70 ± 0.48	-3.10 ± 0.43	3.14 ± 0.42	-0.96 ± 0.42	1.25 ± 0.43	-1.50 ± 0.40	0.55 ± 0.37
11	1.045	1.01 ± 0.42	-1.00 ± 0.37	2.68 ± 0.36	-0.72 ± 0.38	1.19 ± 0.38	-1.08 ± 0.37	0.29 ± 0.35
12	1.271	-0.43 ± 0.38	-1.95 ± 0.35	4.17 ± 0.33	0.39 ± 0.36	2.41 ± 0.36	-1.10 ± 0.36	0.44 ± 0.35

TABLE II: The mean value of M_h (given in GeV) and the final beam spin asymmetries as a function of M_h in each bin for each of the seven azimuthal modulations. Asymmetries are given as

$$100A_{LU}^{\text{stat}}.$$

Bin	$\langle z \rangle$	$A_{LU}^{\sin(\phi_h)}$	$A_{LU}^{\sin(\phi_h - \phi_{R\perp})}$	$A_{LU}^{\sin(\phi_{R\perp})}$	$A_{LU}^{\sin(2\phi_h - \phi_{R\perp})}$	$A_{LU}^{\sin(2\phi_h - 2\phi_{R\perp})}$	$A_{LU}^{\sin(-\phi_h + 2\phi_{R\perp})}$	$A_{LU}^{\sin(3\phi_h - 2\phi_{R\perp})}$
1	0.400	3.13 ± 0.68	-1.38 ± 0.81	1.90 ± 0.78	-1.31 ± 0.67	-1.79 ± 0.83	1.13 ± 0.66	-0.28 ± 0.62
2	0.474	2.52 ± 0.65	0.55 ± 0.89	0.85 ± 0.79	-0.20 ± 0.67	-2.50 ± 0.88	-0.05 ± 0.69	-0.77 ± 0.65
3	0.528	1.96 ± 0.59	3.56 ± 0.86	-0.21 ± 0.74	1.27 ± 0.63	-0.90 ± 0.83	0.13 ± 0.64	0.23 ± 0.61
4	0.579	2.47 ± 0.63	2.39 ± 0.94	0.83 ± 0.79	-0.00 ± 0.68	-1.08 ± 0.89	-0.25 ± 0.69	0.25 ± 0.66
5	0.638	3.90 ± 0.58	1.88 ± 0.89	0.55 ± 0.72	0.04 ± 0.64	-2.43 ± 0.82	0.81 ± 0.64	-0.40 ± 0.61
6	0.727	2.65 ± 0.71	2.34 ± 1.11	-0.71 ± 0.85	-0.03 ± 0.75	-3.07 ± 0.98	1.51 ± 0.75	-1.24 ± 0.69

TABLE III: The mean value of z and the final beam spin asymmetries as a function of z in each bin for $M_h < 0.63$ GeV for each of the seven azimuthal modulations. Asymmetries are given as

$$100A_{LU}^{\text{stat}}.$$

Bin	$\langle z \rangle$	$A_{LU}^{\sin(\phi_h)}$	$A_{LU}^{\sin(\phi_h - \phi_{R\perp})}$	$A_{LU}^{\sin(\phi_{R\perp})}$	$A_{LU}^{\sin(2\phi_h - \phi_{R\perp})}$	$A_{LU}^{\sin(2\phi_h - 2\phi_{R\perp})}$	$A_{LU}^{\sin(-\phi_h + 2\phi_{R\perp})}$	$A_{LU}^{\sin(3\phi_h - 2\phi_{R\perp})}$
1	0.404	1.43 ± 0.70 ± 0.12	-2.33 ± 0.43 ± 0.17	2.27 ± 0.64 ± 0.21	-0.90 ± 0.63 ± 0.09	2.67 ± 0.49 ± 0.21	-2.45 ± 0.58 ± 0.18	0.12 ± 0.55 ± 0.08
2	0.474	1.90 ± 0.67 ± 0.15	-2.66 ± 0.48 ± 0.15	3.81 ± 0.60 ± 0.22	-1.69 ± 0.59 ± 0.19	2.95 ± 0.49 ± 0.19	-1.87 ± 0.55 ± 0.15	-0.86 ± 0.53 ± 0.18
3	0.528	3.00 ± 0.61 ± 0.17	-2.52 ± 0.40 ± 0.12	4.18 ± 0.55 ± 0.21	-0.26 ± 0.40 ± 0.10	3.08 ± 0.45 ± 0.19	-2.82 ± 0.45 ± 0.13	0.64 ± 0.44 ± 0.08
4	0.580	2.87 ± 0.55 ± 0.17	-2.56 ± 0.46 ± 0.11	3.70 ± 0.54 ± 0.22	-0.93 ± 0.58 ± 0.12	3.31 ± 0.49 ± 0.22	-2.92 ± 0.54 ± 0.15	0.18 ± 0.52 ± 0.18
5	0.638	2.70 ± 0.54 ± 0.22	-2.46 ± 0.45 ± 0.11	4.79 ± 0.51 ± 0.22	-1.98 ± 0.52 ± 0.15	3.88 ± 0.46 ± 0.37	-2.28 ± 0.50 ± 0.12	1.59 ± 0.47 ± 0.10
6	0.731	1.40 ± 0.57 ± 0.16	-2.93 ± 0.49 ± 0.11	5.12 ± 0.52 ± 0.26	-1.25 ± 0.51 ± 0.10	1.55 ± 0.46 ± 0.21	-2.92 ± 0.51 ± 0.11	1.21 ± 0.47 ± 0.05

TABLE IV: The mean value of z and the final beam spin asymmetries as a function of z in each bin for $M_h > 0.63$ GeV for each of the seven azimuthal modulations. Asymmetries are given as

$$100A_{LU}^{\text{stat}}_{\text{sys}}.$$

Bin	$\langle P_h^\perp \rangle$	$A_{LU}^{\sin(\phi_h)}$	$A_{LU}^{\sin(\phi_h - \phi_{R\perp})}$	$A_{LU}^{\sin(\phi_{R\perp})}$	$A_{LU}^{\sin(2\phi_h - \phi_{R\perp})}$	$A_{LU}^{\sin(2\phi_h - 2\phi_{R\perp})}$	$A_{LU}^{\sin(-\phi_h + 2\phi_{R\perp})}$	$A_{LU}^{\sin(3\phi_h - 2\phi_{R\perp})}$
1	0.169	0.77 ± 1.11 ± 0.09	0.56 ± 1.47 ± 0.15	1.34 ± 0.88 ± 0.11	1.20 ± 0.93 ± 0.11	-1.77 ± 1.02 ± 0.18	0.74 ± 1.04 ± 0.10	-0.41 ± 0.74 ± 0.05
2	0.311	0.60 ± 1.07 ± 0.09	2.01 ± 1.51 ± 0.24	-0.30 ± 1.19 ± 0.13	-0.70 ± 0.89 ± 0.21	1.53 ± 1.20 ± 0.37	-0.03 ± 0.93 ± 0.09	0.06 ± 0.77 ± 0.04
3	0.426	1.84 ± 0.89 ± 0.15	3.70 ± 1.34 ± 0.36	-0.99 ± 1.09 ± 0.14	0.84 ± 0.79 ± 0.12	-0.58 ± 1.13 ± 0.09	0.41 ± 0.82 ± 0.06	0.11 ± 0.74 ± 0.02
4	0.533	4.10 ± 0.75 ± 0.32	1.55 ± 1.16 ± 0.20	0.80 ± 0.96 ± 0.11	0.65 ± 0.74 ± 0.05	-2.26 ± 1.07 ± 0.16	0.90 ± 0.76 ± 0.09	-0.05 ± 0.73 ± 0.02
5	0.653	3.64 ± 0.56 ± 0.22	0.07 ± 0.88 ± 0.17	2.19 ± 0.73 ± 0.19	-0.81 ± 0.62 ± 0.12	-3.15 ± 0.87 ± 0.18	0.83 ± 0.63 ± 0.07	-0.46 ± 0.63 ± 0.05
6	0.863	2.95 ± 0.41 ± 0.18	1.62 ± 0.61 ± 0.20	0.28 ± 0.52 ± 0.12	-0.81 ± 0.49 ± 0.05	-2.27 ± 0.64 ± 0.10	-0.01 ± 0.49 ± 0.07	-0.34 ± 0.49 ± 0.04

TABLE V: The mean value of P_h^\perp (given in GeV) and the final beam spin asymmetries as a function of P_h^\perp in each bin for $M_h < 0.63$ GeV for each of the seven azimuthal modulations.

$$\text{Asymmetries are given as } 100A_{LU}^{\text{stat}}_{\text{sys}}.$$

Bin	$\langle P_h^\perp \rangle$	$A_{LU}^{\sin(\phi_h)}$	$A_{LU}^{\sin(\phi_h - \phi_{R\perp})}$	$A_{LU}^{\sin(\phi_{R\perp})}$	$A_{LU}^{\sin(2\phi_h - \phi_{R\perp})}$	$A_{LU}^{\sin(2\phi_h - 2\phi_{R\perp})}$	$A_{LU}^{\sin(-\phi_h + 2\phi_{R\perp})}$	$A_{LU}^{\sin(3\phi_h - 2\phi_{R\perp})}$
1	0.160	0.15 ± 0.52	-0.25 ± 0.46	4.86 ± 0.39	-0.07 ± 0.45	1.24 ± 0.39	-0.71 ± 0.50	1.09 ± 0.41
2	0.306	0.13 ± 0.58	-1.46 ± 0.47	4.73 ± 0.48	-0.86 ± 0.50	1.88 ± 0.43	-2.21 ± 0.50	0.58 ± 0.44
3	0.422	2.22 ± 0.56	-1.76 ± 0.46	4.77 ± 0.56	0.09 ± 0.55	1.08 ± 0.47	-2.26 ± 0.53	0.68 ± 0.47
4	0.530	2.49 ± 0.80	-2.80 ± 0.55	3.30 ± 0.76	-2.59 ± 0.67	3.66 ± 0.60	-2.69 ± 0.63	0.37 ± 0.57
5	0.648	4.01 ± 0.94	-2.76 ± 0.59	2.75 ± 0.80	-0.92 ± 0.56	4.92 ± 0.62	-3.04 ± 0.56	1.66 ± 0.63
6	0.852	2.77 ± 1.12	-2.91 ± 0.63	-0.05 ± 1.04	-2.84 ± 0.87	8.13 ± 0.74	-3.58 ± 0.85	1.48 ± 0.75

TABLE VI: The mean value of P_h^\perp and the final beam spin asymmetries as a function of P_h^\perp in each bin for $M_h > 0.63$ GeV for each of the seven azimuthal modulations. Asymmetries are given

as $100A_{LU}^{\text{stat}}_{\text{sys}}$.

II. BIN DEFINITIONS AND MEAN KINEMATIC VALUES

The bin edges for the x , M_h , z and P_h^\perp asymmetries are reported in Tables VII-VIII. In Tables IX-XIV the mean values of x , Q^2 , M_h , z , P_h^\perp , θ , K_2 and K_3 are reported for each bin. Figs. 1-4 show plots of seven asymmetry amplitudes for each binning scheme.

Bin	x	M_h (GeV)
1	(0.000, 0.118]	(0.270, 0.381]
2	(0.118, 0.135]	(0.381, 0.462]
3	(0.135, 0.150]	(0.462, 0.531]
4	(0.150, 0.165]	(0.531, 0.606]
5	(0.165, 0.183]	(0.606, 0.675]
6	(0.183, 0.200]	(0.675, 0.737]
7	(0.200, 0.223]	(0.737, 0.781]
8	(0.223, 0.248]	(0.781, 0.831]
9	(0.248, 0.275]	(0.831, 0.900]
10	(0.275, 0.315]	(0.900, 0.981]
11	(0.315, 0.375]	(0.981, 1.125]
12	(0.375, 1.000]	(1.125, 2.500]

TABLE VII: Bins of the 1-D projections of the A_{LU} measurements for the variables x and M_h .

Bin	z	P_h^\perp (GeV)
1	(0.000, 0.445]	(0.000, 0.245]
2	(0.445, 0.500]	(0.245, 0.365]
3	(0.500, 0.555]	(0.365, 0.480]
4	(0.555, 0.605]	(0.480, 0.585]
5	(0.605, 0.675]	(0.585, 0.725]
5	(0.675, 1.000]	(0.725, 1.500]

TABLE VIII: Bins of the 2-D projections of the A_{LU} measurements for the variables z and P_h^\perp .

The asymmetries are determined for $M_h < 0.63$ GeV and $M_h > 0.63$ GeV.

Bin	$\langle x \rangle$	$\langle Q^2 \rangle$ (GeV 2)	$\langle M_h \rangle$ (GeV)	$\langle z \rangle$	$\langle P_h^\perp \rangle$ (GeV)	$\langle \theta \rangle$	$\langle K_2 \rangle$	$\langle K_3 \rangle$
1	0.105	1.542	0.830	0.531	0.550	1.563	0.874	0.699
2	0.127	1.783	0.809	0.547	0.530	1.569	0.842	0.692
3	0.143	1.953	0.794	0.557	0.526	1.567	0.822	0.685
4	0.157	2.105	0.780	0.559	0.520	1.575	0.805	0.679
5	0.174	2.286	0.763	0.566	0.506	1.575	0.793	0.673
6	0.191	2.471	0.749	0.571	0.500	1.574	0.780	0.668
7	0.211	2.707	0.743	0.571	0.492	1.575	0.776	0.665
8	0.235	3.003	0.733	0.572	0.485	1.576	0.776	0.664
9	0.261	3.307	0.716	0.571	0.468	1.578	0.771	0.662
10	0.294	3.721	0.701	0.569	0.460	1.578	0.773	0.663
11	0.342	4.337	0.679	0.565	0.444	1.585	0.778	0.665
12	0.441	5.658	0.630	0.547	0.408	1.588	0.796	0.674

TABLE IX: Average kinematic values for the 1-D x bins. K_2 (K_3) denotes the twist-2 (twist-3) y -dependent kinematic depolarization factor entering the two-pion production cross section.

Bin	$\langle x \rangle$	$\langle Q^2 \rangle$ (GeV 2)	$\langle M_h \rangle$ (GeV)	$\langle z \rangle$	$\langle P_h^\perp \rangle$ (GeV)	$\langle \theta \rangle$	$\langle K_2 \rangle$	$\langle K_3 \rangle$
1	0.249	3.145	0.338	0.530	0.638	1.640	0.778	0.664
2	0.242	3.090	0.422	0.546	0.589	1.600	0.785	0.668
3	0.240	3.057	0.496	0.551	0.571	1.576	0.785	0.668
4	0.238	3.056	0.568	0.555	0.549	1.571	0.789	0.671
5	0.233	3.000	0.641	0.547	0.519	1.572	0.793	0.671
6	0.225	2.918	0.708	0.550	0.494	1.575	0.796	0.673
7	0.222	2.893	0.759	0.555	0.472	1.575	0.796	0.673
8	0.219	2.855	0.805	0.559	0.458	1.572	0.798	0.673
9	0.216	2.826	0.864	0.560	0.434	1.567	0.801	0.676
10	0.209	2.764	0.939	0.569	0.417	1.560	0.805	0.677
11	0.199	2.665	1.045	0.579	0.394	1.559	0.816	0.680
12	0.180	2.471	1.271	0.628	0.378	1.547	0.832	0.687

TABLE X: Average kinematic values for the 1-D M_h bins. K_2 (K_3) denotes the twist-2 (twist-3) y -dependent kinematic depolarization factor entering the two-pion production cross section.

Bin	$\langle x \rangle$	$\langle Q^2 \rangle$ (GeV 2)	$\langle M_h \rangle$ (GeV)	$\langle z \rangle$	$\langle P_h^\perp \rangle$ (GeV)	$\langle \theta \rangle$	$\langle K_2 \rangle$	$\langle K_3 \rangle$
1	0.220	3.129	0.464	0.400	0.598	1.578	0.861	0.696
2	0.244	3.210	0.468	0.474	0.610	1.583	0.809	0.683
3	0.248	3.131	0.472	0.528	0.608	1.581	0.780	0.669
4	0.254	3.107	0.470	0.579	0.590	1.593	0.756	0.655
5	0.253	3.021	0.478	0.638	0.556	1.609	0.739	0.647
6	0.234	2.825	0.482	0.727	0.500	1.627	0.7941	0.650

TABLE XI: Average kinematic values for the 2-D z bins corresponding to $M_h < 0.63$ GeV. K_2 (K_3) denotes the twist-2 (twist-3) y -dependent kinematic depolarization factor entering the two-pion production cross section.

Bin	$\langle x \rangle$	$\langle Q^2 \rangle$ (GeV 2)	$\langle M_h \rangle$ (GeV)	$\langle z \rangle$	$\langle P_h^\perp \rangle$ (GeV)	$\langle \theta \rangle$	$\langle K_2 \rangle$	$\langle K_3 \rangle$
1	0.192	2.764	0.821	0.404	0.386	1.575	0.867	0.698
2	0.209	2.847	0.859	0.474	0.427	1.574	0.830	0.688
3	0.218	2.862	0.880	0.528	0.451	1.573	0.805	0.677
4	0.223	2.850	0.900	0.580	0.466	1.566	0.786	0.669
5	0.221	2.785	0.921	0.638	0.467	1.559	0.773	0.662
6	0.202	2.628	0.958	0.731	0.438	1.551	0.794	0.671

TABLE XII: Average kinematic values for the 2-D z bins corresponding to $M_h > 0.63$ GeV. K_2 (K_3) denotes the twist-2 (twist-3) y -dependent kinematic depolarization factor entering the two-pion production cross section.

Bin	$\langle x \rangle$	$\langle Q^2 \rangle$ (GeV 2)	$\langle M_h \rangle$ (GeV)	$\langle z \rangle$	$\langle P_h^\perp \rangle$ (GeV)	$\langle \theta \rangle$	$\langle K_2 \rangle$	$\langle K_3 \rangle$
1	0.309	3.534	0.501	0.591	0.169	1.587	0.701	0.634
2	0.284	3.429	0.493	0.568	0.311	1.588	0.745	0.651
3	0.259	3.221	0.481	0.553	0.426	1.594	0.766	0.660
4	0.244	3.123	0.474	0.541	0.533	1.590	0.785	0.668
5	0.231	3.027	0.464	0.532	0.653	1.594	0.799	0.675
6	0.204	2.759	0.454	0.531	0.863	1.598	0.823	0.685

TABLE XIII: Average kinematic values for the 2-D P_h^\perp bins corresponding to $M_h < 0.63$ GeV. K_2 (K_3) denotes the twist-2 (twist-3) y -dependent kinematic depolarization factor entering the two-pion production cross section.

Bin	$\langle x \rangle$	$\langle Q^2 \rangle$ (GeV 2)	$\langle M_h \rangle$ (GeV)	$\langle z \rangle$	$\langle P_h^\perp \rangle$ (GeV)	$\langle \theta \rangle$	$\langle K_2 \rangle$	$\langle K_3 \rangle$
1	0.226	2.897	0.946	0.560	0.160	1.556	0.789	0.670
2	0.221	2.865	0.915	0.566	0.306	1.556	0.796	0.673
3	0.217	2.837	0.894	0.570	0.422	1.563	0.801	0.676
4	0.207	2.752	0.876	0.570	0.530	1.570	0.811	0.679
5	0.199	2.677	0.858	0.574	0.648	1.572	0.819	0.684
6	0.182	2.528	0.832	0.586	0.852	1.589	0.839	0.689

TABLE XIV: Average kinematic values for the 2-D P_h^\perp bins corresponding to $M_h > 0.63$ GeV. K_2 (K_3) denotes the twist-2 (twist-3) y -dependent kinematic depolarization factor entering the two-pion production cross section.

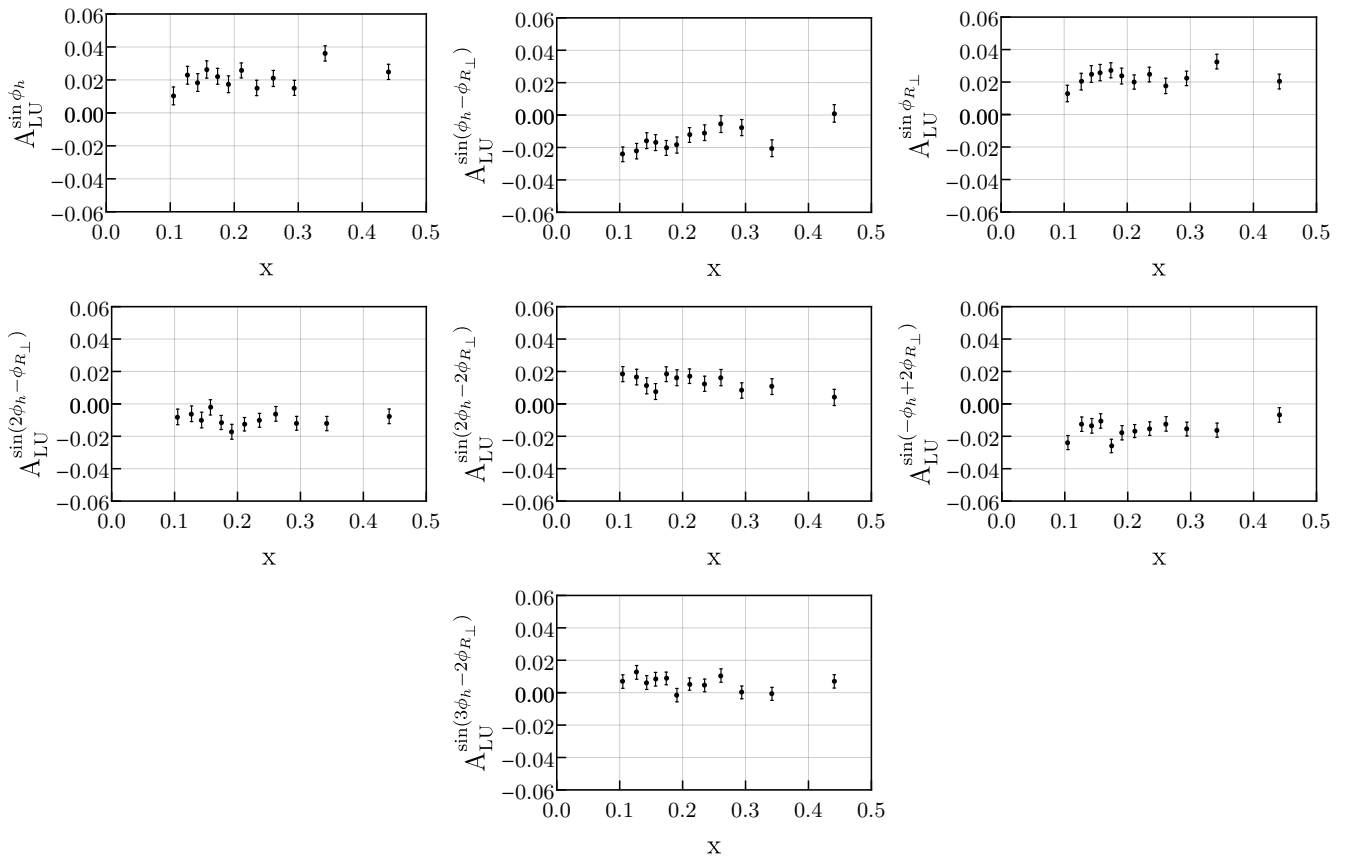


FIG. 1: The seven extracted beam spin asymmetries from the simultaneous fit to all modulations as a function of x . Error bars are purely statistical.

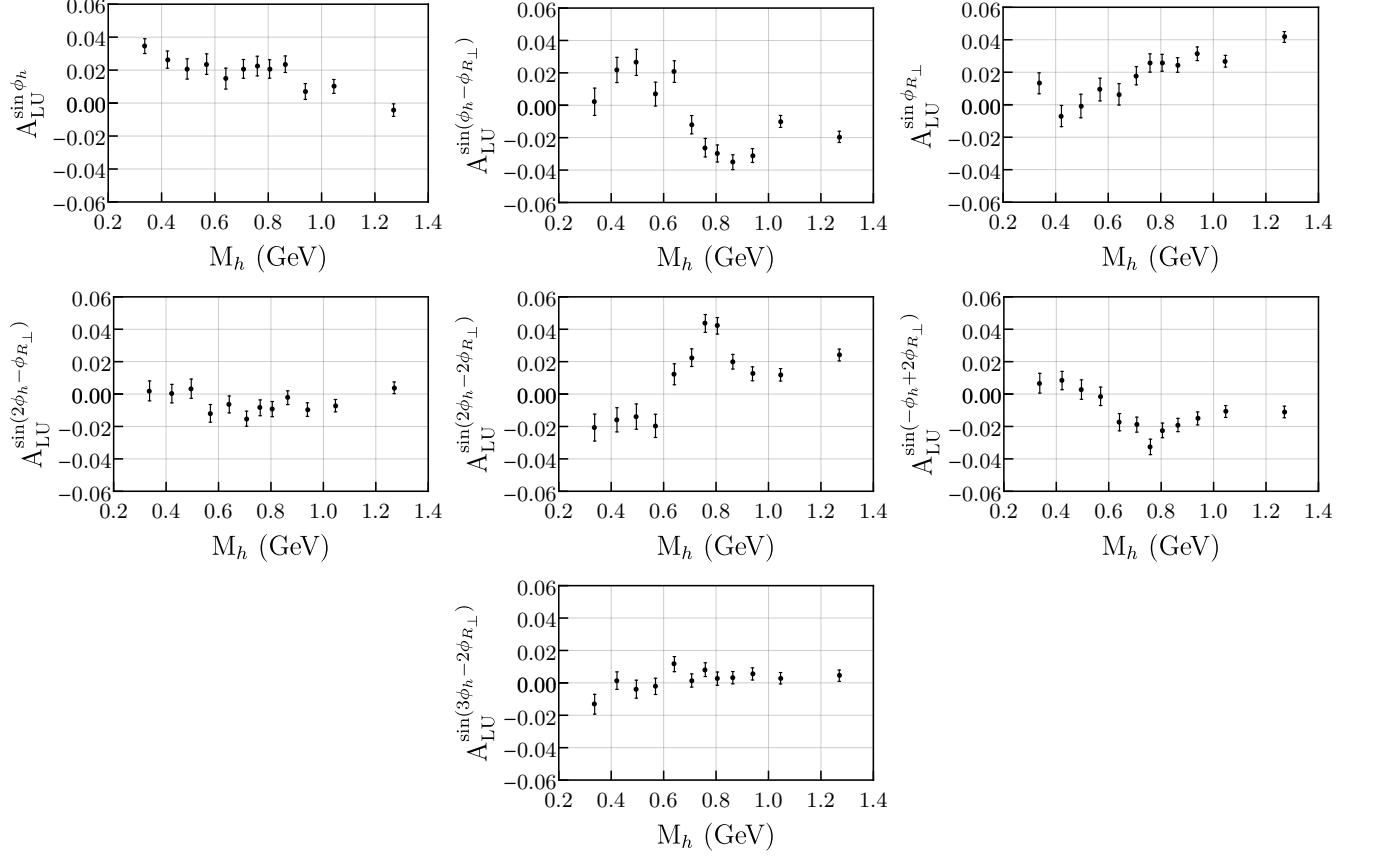


FIG. 2: The seven extracted beam spin asymmetries from the simultaneous fit to all modulations as a function of M_h . Error bars are purely statistical.

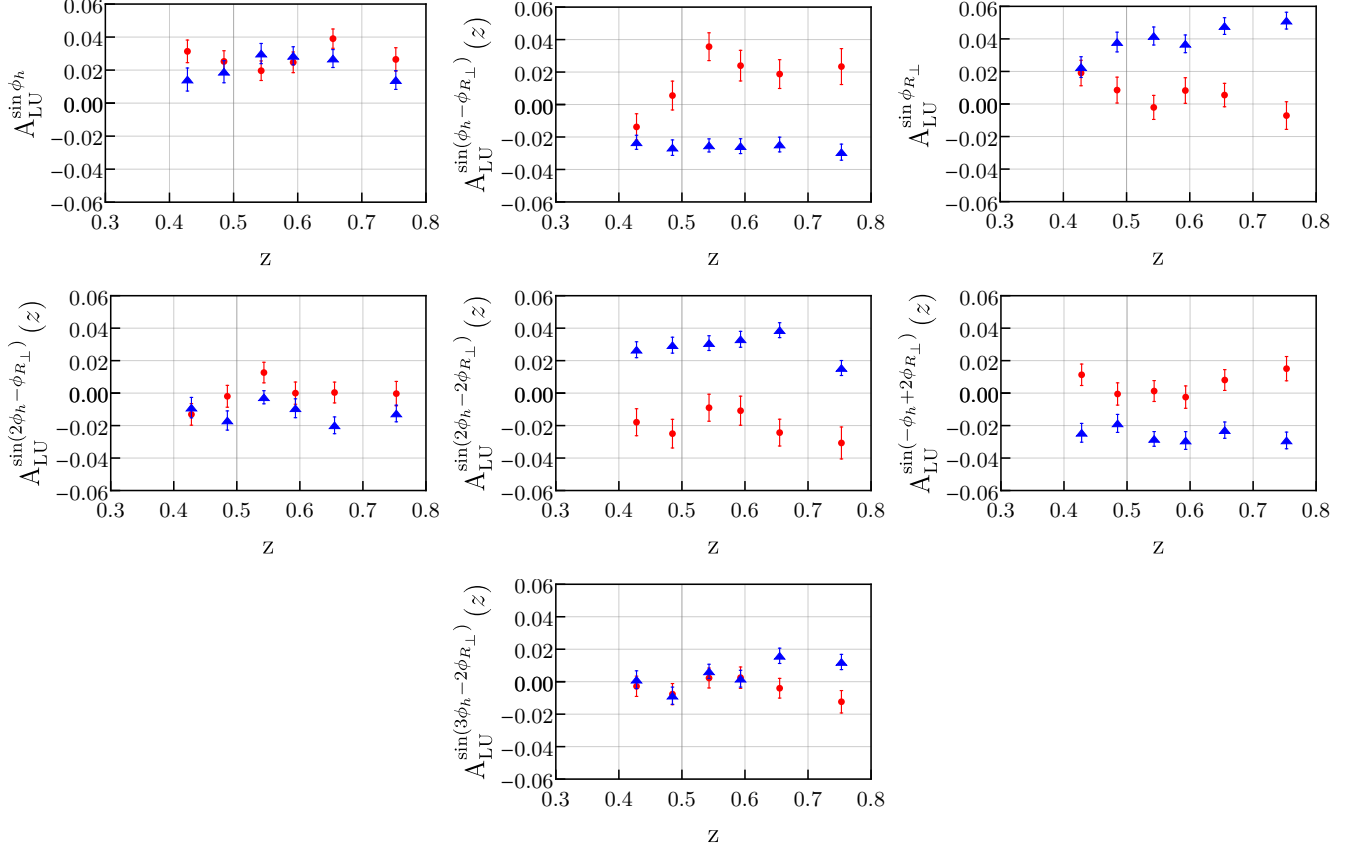


FIG. 3: The seven extracted beam spin asymmetries from the simultaneous fit to all modulations as a function of z for $M_h < 0.63$ GeV (red circles) and $M_h > 0.63$ GeV (blue triangles). Error bars are purely statistical.

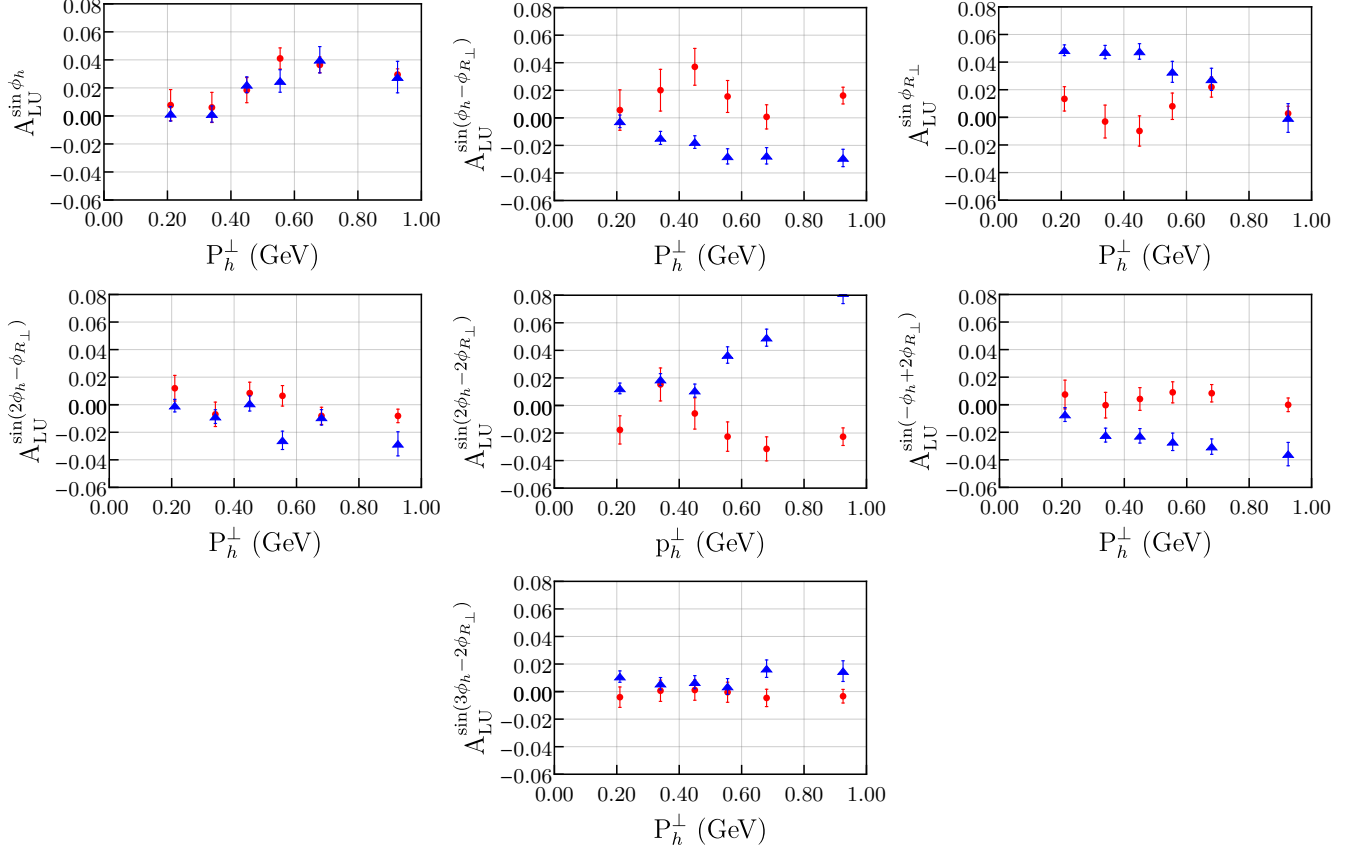


FIG. 4: The seven extracted beam spin asymmetries from the simultaneous fit to all modulations as a function of P_h^\perp (given in GeV) for $M_h < 0.63$ GeV (red circles) and $M_h > 0.63$ GeV (blue triangles). Error bars are purely statistical.

III. INFLUENCE ON A_{LU} FROM UNPOLARIZED CROSS SECTION MODULATIONS

The unpolarized cross section $d\sigma_{UU}$, which resides in the denominator of A_{LU} , also contains several modulations [3]. Limitations in the CLAS12 acceptance introduce linear dependence between the amplitudes, hence A_{LU} could be influenced by nonzero amplitudes of $d\sigma_{UU}$ modulations. These amplitudes have not yet been measured for the relevant kinematical ranges, therefore it is difficult to correct for their impact. Instead, we assume they are no more than 10% and performed a Monte Carlo study to assess their influence on the final A_{LU} values. Figs. 5-10 show distributions of δ , the resulting shift on an A_{LU} amplitude from nonzero $d\sigma_{UU}$ amplitudes, for each A_{LU} measurement bin. In general, $\delta \lesssim 0.3\%$.

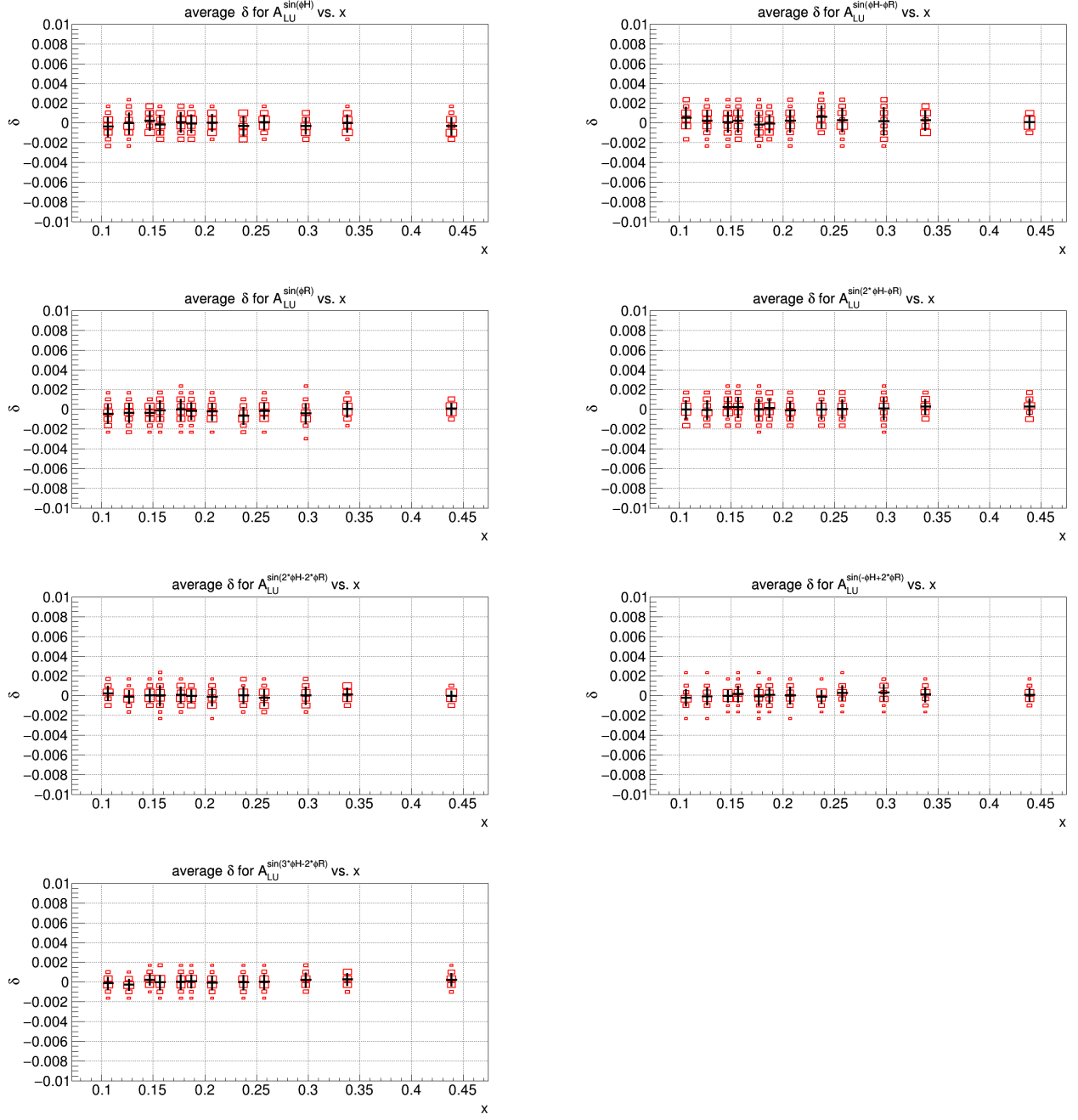


FIG. 5: Distribution of δ for each kinematic bin and σ_{LU} modulation; this is for the binning in x . One histogram entry (red box plot) corresponds to one σ_{UU} amplitude injection; the size of the red box is proportional to the number of entries in that bin. The black crosses indicate the mean δ for each kinematic bin, and the vertical size of the black cross indicates the standard deviation of δ .

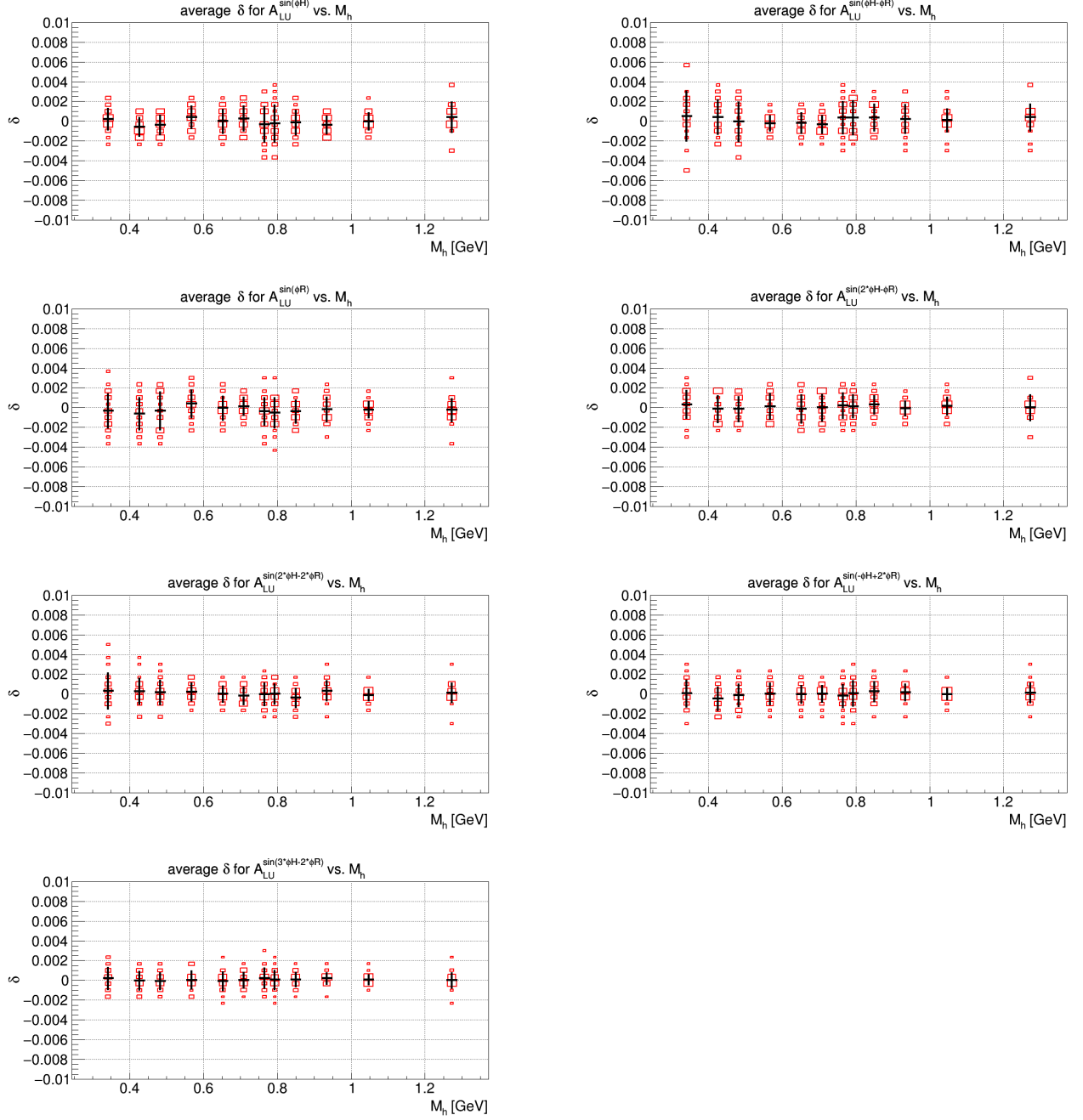


FIG. 6: Distribution of δ for each kinematic bin and σ_{LU} modulation; this is for the binning in M_h . One histogram entry (red box plot) corresponds to one σ_{UU} amplitude injection; the size of the red box is proportional to the number of entries in that bin. The black crosses indicate the mean δ for each kinematic bin, and the vertical size of the black cross indicates the standard deviation of δ .

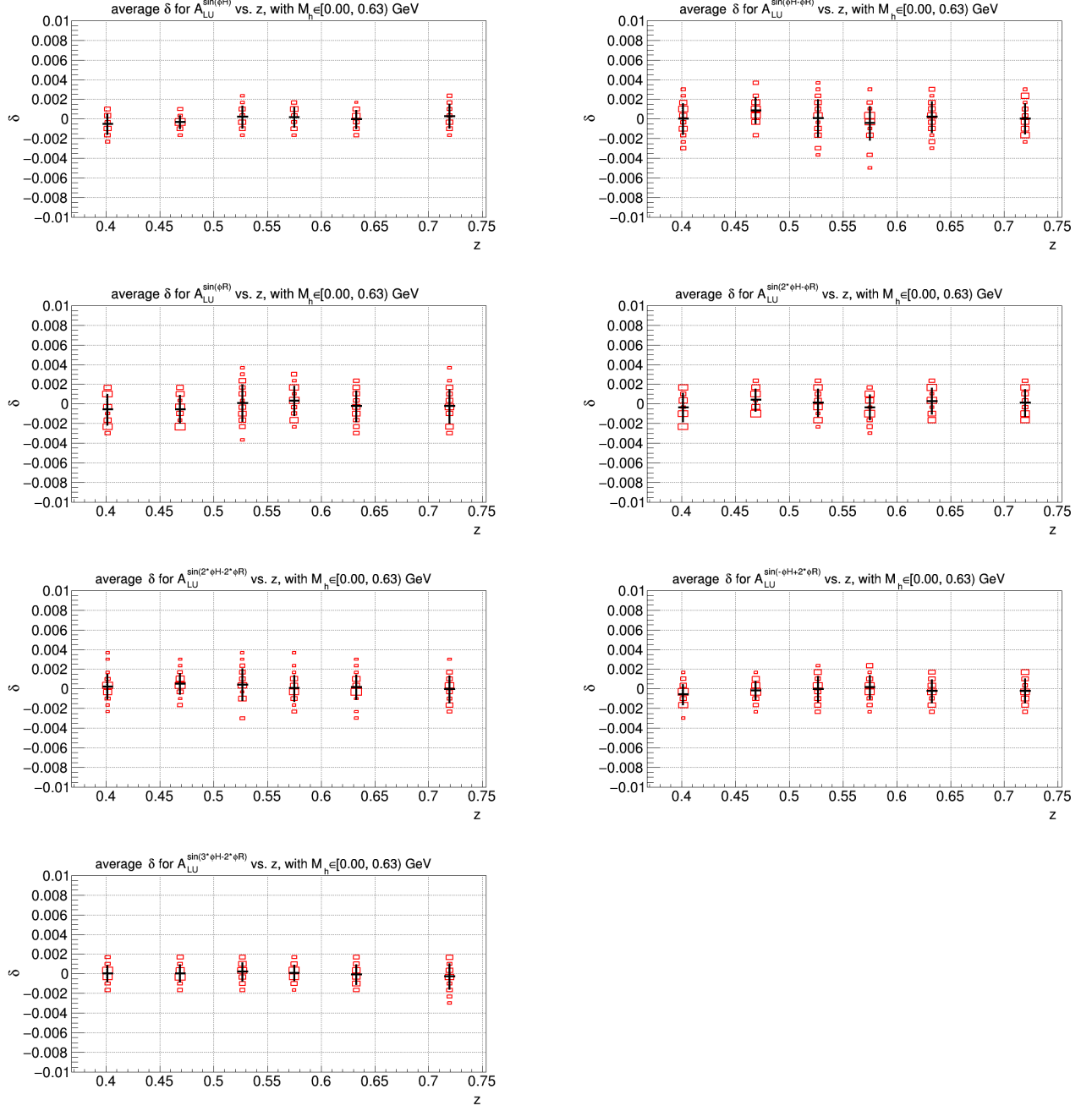


FIG. 7: Distribution of δ for each kinematic bin and σ_{LU} modulation; this is for the binning in z , with $M_h < 0.63$ GeV. One histogram entry (red box plot) corresponds to one σ_{UU} amplitude injection; the size of the red box is proportional to the number of entries in that bin. The black crosses indicate the mean δ for each kinematic bin, and the vertical size of the black cross indicates the standard deviation of δ .

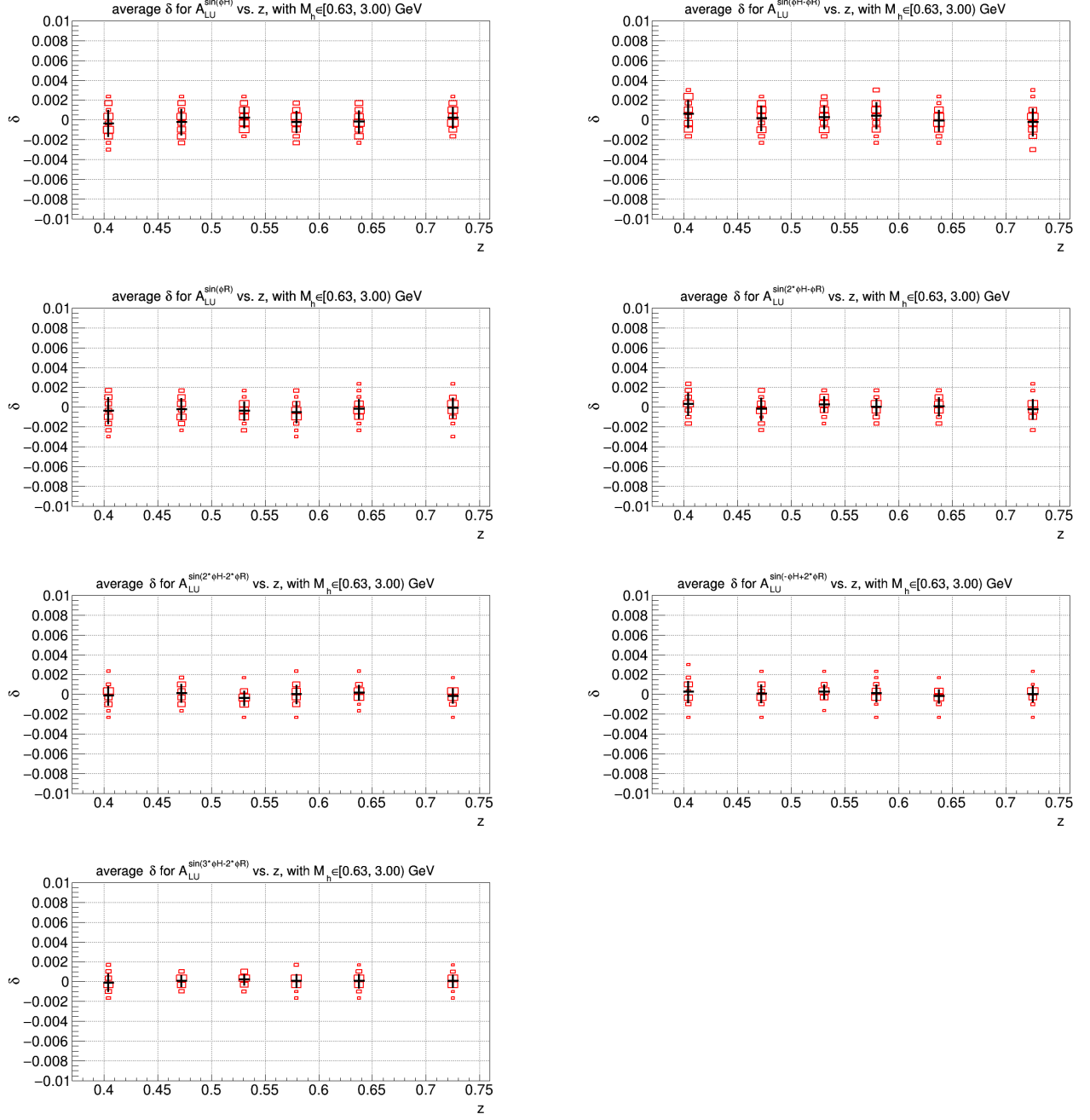


FIG. 8: Distribution of δ for each kinematic bin and σ_{LU} modulation; this is for the binning in z , with $M_h > 0.63$ GeV. One histogram entry (red box plot) corresponds to one σ_{UU} amplitude injection; the size of the red box is proportional to the number of entries in that bin. The black crosses indicate the mean δ for each kinematic bin, and the vertical size of the black cross indicates the standard deviation of δ .

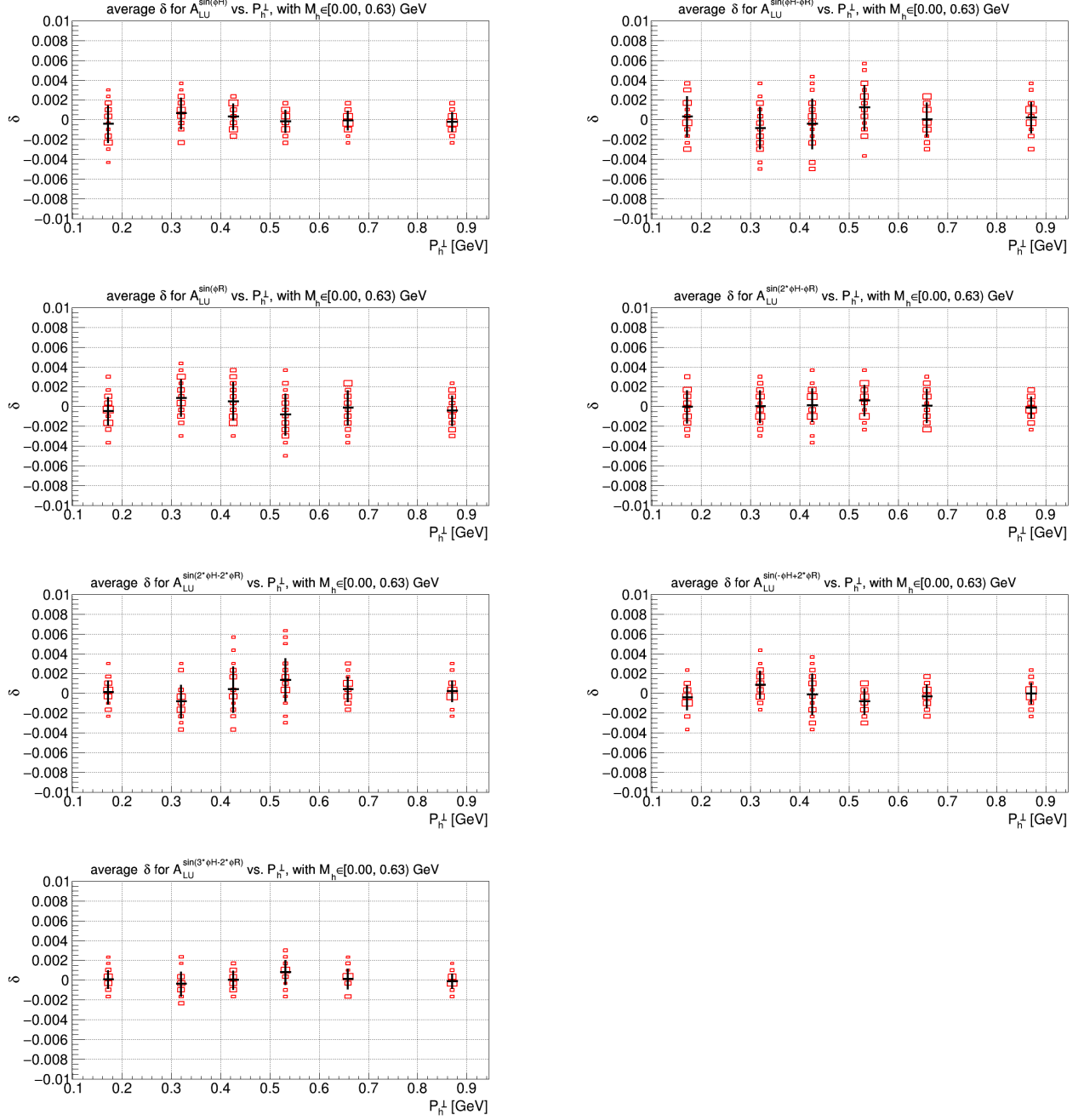


FIG. 9: Distribution of δ for each kinematic bin and σ_{LU} modulation; this is for the binning in P_h^\perp , with $M_h < 0.63$ GeV. One histogram entry (red box plot) corresponds to one σ_{UU} amplitude injection; the size of the red box is proportional to the number of entries in that bin. The black crosses indicate the mean δ for each kinematic bin, and the vertical size of the black cross indicates the standard deviation of δ .

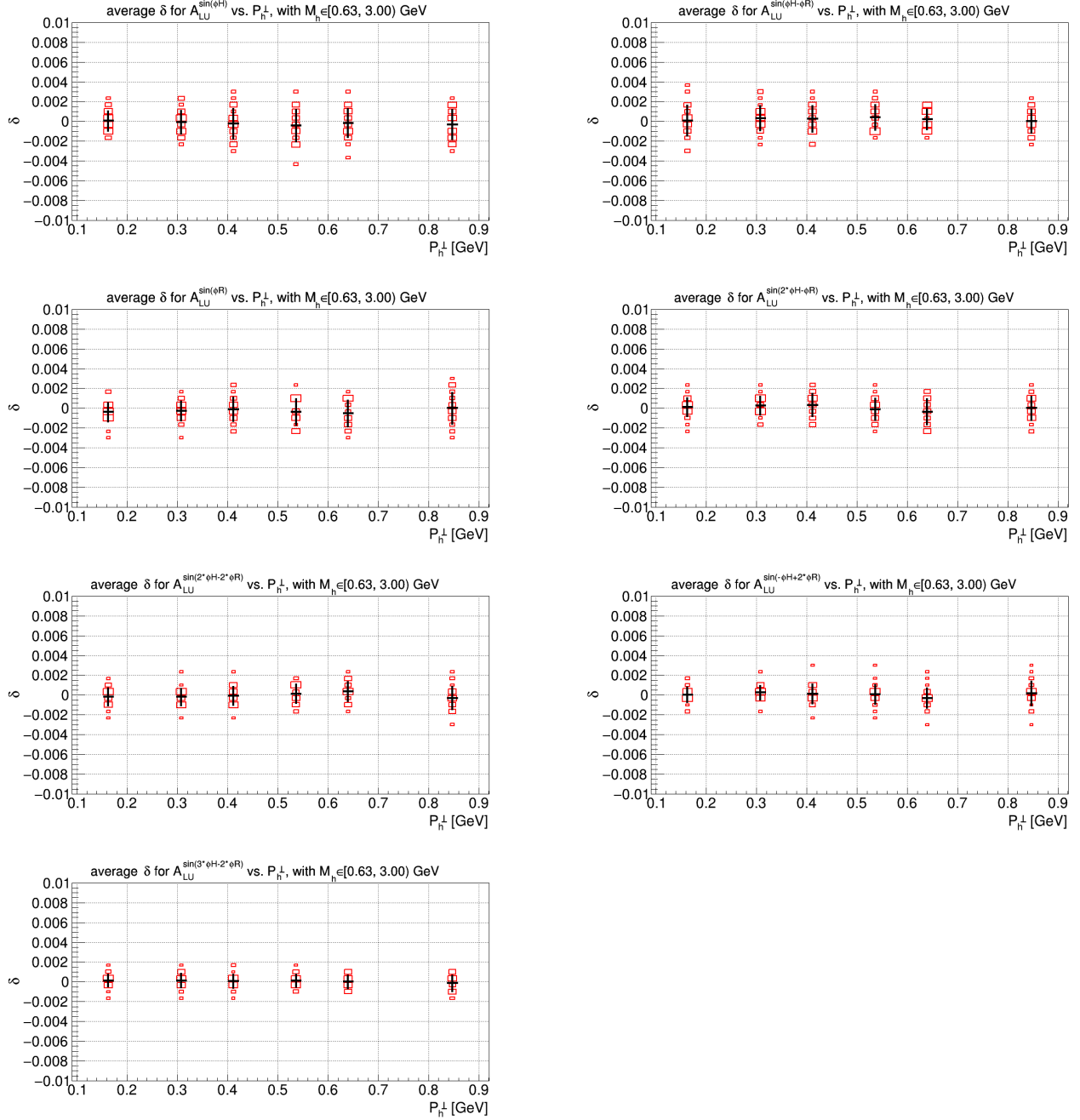


FIG. 10: Distribution of δ for each kinematic bin and σ_{LU} modulation; this is for the binning in P_h^\perp , with $M_h > 0.63$ GeV. One histogram entry (red box plot) corresponds to one σ_{UU} amplitude injection; the size of the red box is proportional to the number of entries in that bin. The black crosses indicate the mean δ for each kinematic bin, and the vertical size of the black cross indicates the standard deviation of δ .

IV. CORRECTING FOR THE $P_{2,0}$ MODULATION OF THE UNPOLARIZED CROSS SECTION

The full partial wave expansion of the dihadron cross section also includes modulations in θ , the dihadron frame decay angle. The modulation $P_{2,0}(\cos \theta) = (3 \cos^2 \theta - 1)/2$ of $d\sigma_{UU}$ is of particular importance and has been studied in other measurements, such as those from HERMES [4], where they employed a similar strategy as our aforementioned Monte Carlo study. Since this modulation is dependent only on θ and not on ϕ_h or ϕ_{R_\perp} , we find the shift δ on A_{LU} to be

$$\delta = \frac{AB\langle P_{2,0} \rangle}{1 + B\langle P_{2,0} \rangle}, \quad (6)$$

where A is the original A_{LU} amplitude, B is the amplitude of $P_{2,0}$, and $\langle P_{2,0} \rangle$ is the mean value of $P_{2,0}$ from the data. Tables XV-XX give the value of $\langle P_{2,0} \rangle$ for each kinematic bin used in the asymmetry analysis. When a proper measurement of the amplitude of this modulation becomes available, Eq. 6 can be used in combination with the values listed in these tables in order to correct the presented A_{LU} values.

Bin	$\langle x \rangle$	$\langle P_{2,0}(\cos \theta) \rangle$
1	0.105	-0.404
2	0.127	-0.408
3	0.143	-0.410
4	0.157	-0.412
5	0.174	-0.414
6	0.191	-0.417
7	0.211	-0.418
8	0.235	-0.419
9	0.261	-0.419
10	0.294	-0.419
11	0.342	-0.419
12	0.441	-0.419

TABLE XV: Mean values of $P_{2,0}(\cos \theta)$ for the binning scheme in x .

Bin	$\langle M_h \rangle$ (GeV)	$\langle P_{2,0}(\cos \theta) \rangle$
1	0.338	-0.338
2	0.422	-0.409
3	0.496	-0.420
4	0.568	-0.426
5	0.641	-0.428
6	0.708	-0.429
7	0.759	-0.427
8	0.805	-0.426
9	0.864	-0.425
10	0.939	-0.422
11	1.045	-0.417
12	1.271	-0.404

TABLE XVI: Mean values of $P_{2,0}(\cos \theta)$ for the binning scheme in M_h .

Bin	$\langle z \rangle$	$\langle P_{2,0}(\cos \theta) \rangle$
1	0.400	-0.461
2	0.474	-0.430
3	0.528	-0.409
4	0.579	-0.390
5	0.638	-0.368
6	0.727	-0.325

TABLE XVII: Mean values of $P_{2,0}(\cos \theta)$ for the binning scheme in z , with $M_h < 0.63$ GeV.

Bin	$\langle z \rangle$	$\langle P_{2,0}(\cos \theta) \rangle$
1	0.404	-0.477
2	0.474	-0.456
3	0.528	-0.440
4	0.580	-0.424
5	0.638	-0.403
6	0.731	-0.354

TABLE XVIII: Mean values of $P_{2,0}(\cos \theta)$ for the binning scheme in z , with $M_h > 0.63$ GeV.

Bin	$\langle P_h^\perp \rangle$ (GeV)	$\langle P_{2,0}(\cos \theta) \rangle$
1	0.169	-0.427
2	0.311	-0.420
3	0.426	-0.414
4	0.533	-0.408
5	0.653	-0.400
6	0.863	-0.379

TABLE XIX: Mean values of $P_{2,0}(\cos \theta)$ for the binning scheme in P_h^\perp , with $M_h < 0.63$ GeV.

Bin	$\langle P_h^\perp \rangle$ (GeV)	$\langle P_{2,0}(\cos \theta) \rangle$
1	0.160	-0.434
2	0.306	-0.428
3	0.422	-0.424
4	0.530	-0.418
5	0.648	-0.413
6	0.852	-0.402

TABLE XX: Mean values of $P_{2,0}(\cos \theta)$ for the binning scheme in P_h^\perp , with $M_h > 0.63$ GeV.

-
- [1] A. Bacchetta and M. Radici, Phys. Rev. D **67**, 094002 (2003), arXiv:hep-ph/0212300.
 - [2] A. Bacchetta and M. Radici, Phys. Rev. D **69**, 074026 (2004), arXiv:hep-ph/0311173.
 - [3] S. Gliske, A. Bacchetta, and M. Radici, Phys. Rev. D **90**, 114027 (2014), [Erratum: Phys.Rev.D 91, 019902 (2015)], arXiv:1408.5721 [hep-ph].
 - [4] A. Airapetian *et al.* (HERMES Collaboration), JHEP **06**, 017 (2008), arXiv:0803.2367 [hep-ex].